Transport and physical properties of V_2O_5–P_2O_5–B_2O_3 glasses doped with Dy_2O_3

R. V. BARDE

Department of Engineering Physics, Shri Hanuman Vyayam Prasarak Mandal's College of Engineering and Technology, Amravati 444 605, India

S. A. WAGHULEY

Department of Physics, Sant Gadge Baba Amravati University, Amravati 444 602, India

Research Article

Transport and physical properties of V_2O_5–P_2O_5–B_2O_3 glasses doped with Dy_2O_3

R. V. BARDE[a], S. A. WAGHULEY[b,*]

aDepartment of Engineering Physics, Shri Hanuman Vyayam Prasarak Mandal's College of Engineering and Technology, Amravati 444 605, India
bDepartment of Physics, Sant Gadge Baba Amravati University, Amravati 444 602, India

Abstract: We investigate the DC transport properties of $60V_2O_5$–$5P_2O_5$–$(35-x)B_2O_3$–xDy_2O_3 (x = 0.4, 0.6, 0.8, 1.0 and 1.2 mol%) glasses as function of temperature which were prepared using the conventional melt-quenching method. These glasses are characterised by thermo gravimetric-differential thermal analysis (TG-DTA). Activation energy (E_{DC}) is obtained from Arrhenius plots of temperature-dependent DC conductivity, and it is found to be 0.30 eV for high conducting glass. In order to understand the role of Dy_2O_3 in these glasses, the density and molar volume are investigated. The results show that molar volume of the glass increases with the increasing of Dy_2O_3 concentration. The ionic conductivity is found to be dominant over the electronic conductivity and varies between 82% and 96%.

Keywords: transport properties; melt quenching; Arrhenius plot; glasses

1 Introduction

Transition metal oxide glasses have been studied because of their interesting semiconducting properties, which are due to the hopping of "polarons" from the higher to the lower valence states of the transition metal ions [1]. In these glasses, strong electron–phonon interaction is responsible for the formation of small polarons [2,3]. Vanadate glasses contain V^{4+} and V^{5+} ions, where the electrical conduction is endorsed to the hopping of $3d^1$ unpaired electron from V^{4+} to V^{5+} sites. These glasses have been considered as a new branch in semiconducting glasses because of their wider glass-forming region and possible technological applications [4–8]. In B_2O_3 glasses, two groups of bands such as trigonal BO_3 and tetrahedral BO_4 are obtained [9]. When transition metal ions are added to the borate glasses, they exhibit specific physical properties. When these glasses are grafted with alkaline earth ions, the resultant glasses have several applications [10–13]. Phosphate glasses hold abundant advantages such as high thermal conductivity, low melting and softening temperature and high thermal expansion coefficient over silicate and borate glasses [14].

In the last three decades, several attempts were made to develop fast ion conducting glasses because of their prospective applications as high energy density batteries [15]. The physical properties of the phosphate glasses can be improved by the addition of different heavy metal oxides [16,17].

Glasses containing rare earth and transition metal

---
* Corresponding author.
E-mail: sandeepwaghuley@sgbau.ac.in

have been widely studied using structural and optical spectroscopy due to their many potential applications, like optical amplifiers in telecommunication [18], phosphorescence materials and electrochemical batteries [19].

The aim of this work is to prepare the glass systems $60V_2O_5$–$5P_2O_5$–$(35–x)B_2O_3$–xDy_2O_3 ($x = 0.4$, 0.6, 0.8, 1.0 and 1.2 mol%) to analyze the DC electrical, thermal and physical properties. The characterization technique, thermo gravimetric-differential thermal analysis (TG-DTA) is employed to study the structural properties of the glass samples.

2 Experiment

The preparation of $60V_2O_5$–$5P_2O_5$–$(35–x)B_2O_3$–xDy_2O_3 ($x = 0.4$, 0.6, 0.8, 1.0 and 1.2 mol%) glasses has been described and its characterization details were reported in Ref. [20]. For the electrical measurements, the samples were polished and conducting silver paste was deposited on both sides. The sample area was taken to be the area exposed to the electrode surface. The area under electrode ranged between 0.22–0.33 cm^2, and the thickness of samples varied between 0.29–0.36 cm. Measurements of DC conductivity as a function of temperature in all the samples were made by two-probe technique in the temperature range of 303–473 K, as the glass systems $60V_2O_5$–$5P_2O_5$–$(35–x)B_2O_3$–xDy_2O_3 have low Johnson noise due to high conductance at high temperature [21]. For ionic transference number measurement, the samples were polished and graphite electrode (blocking electrode) was deposited on both sides of the samples. The samples were held between the sample holders. The sample holder was provided with spring-mechanical pressure to ensure good electrical contact. A constant voltage (DC) of 6 V was applied to the samples. The measurement was performed at room temperature. The total ionic (t_{ion}) and electronic (t_{ele}) transference numbers were calculated from Eqs. (1) and (2) [22–25]:

$$t_{ion} = \frac{I_i - I_f}{I_i} \qquad (1)$$

$$t_{ele} = 100 - t_{ion} \qquad (2)$$

where I_i is the initial value of the current at the start; and I_f is the current on reaching saturation.

The density of the glass bits free of air bubbles and cracks was determined at room temperature through Archimedes principle, by using xylene ($\rho = 0.863$ g/ml). The density was estimated by using Eq. (3):

$$\rho = \left(\frac{W_a}{W_a - W_l} \right) \times \rho_l \qquad (3)$$

where ρ is the density of the sample; W_a is the weight of the sample in air; W_l is the weight of the sample fully immersed in xylene; and ρ_l is the density of xylene.

The molar volume V_m was calculated from Eq. (4) [26–30]:

$$V_m = \frac{M_T}{\rho} \qquad (4)$$

where M_T is the molecular weight of the glass calculated by multiplying x times the molecular weights of the various constituents.

The oxygen packing density (OPD) was determined from Eq. (5) [31]:

$$D_0 = \left(\frac{\rho}{M_T} \right) \times \text{number of oxygen atoms per formula unit} \qquad (5)$$

3 Results and discussion

3.1 Characterization of materials

From the previous results by X-ray diffraction analysis, it is found that all the samples possess the amorphous nature; the thermal stability was studied by thermo gravimetric differential analysis, and the thermal stability of the glass is found to be excellent for the composition with $x = 0.6$ [20].

3.2 DC conductivity

The DC conductivity (σ_{DC}) for all samples was calculated using the sample dimensions. The reciprocal temperature dependence of the DC conductivity is shown in Fig. 1. The plots show DC conductivity exhibits an Arrhenius-type temperature dependence given by the relation:

$$\sigma_{DC} = \sigma_0 \exp\left(-\frac{E_{DC}}{KT} \right) \qquad (6)$$

where E_{DC} is the activation energy which is calculated from the least square straight line fitting of plots; and σ_0 is the pre-exponential factor.
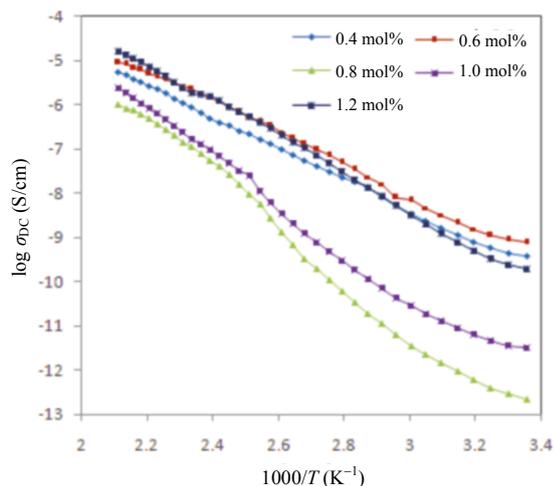
Fig. 1 Temparature dependence of DC conductivity.

Fig. 2 Variation of σ_{DC} and E_{DC} with molar fraction of Dy_2O_3.

The variation of σ_{DC} and E_{DC} as functions of molar fraction of Dy_2O_3 are depicted in Fig. 2. It is observed that the conductivity shows a random nature. At room temperature, it is maximum for 0.6 mol% of Dy_2O_3 and decreases for 0.8 mol% of Dy_2O_3. If we further increase the molar fraction of Dy_2O_3, the conductivity increases. The highest conductivity is found to be 8.22×10^{-3} S/cm at 473 K. The value of activation energy ranges between 0.30–0.52 eV. The maximum value of conductivity corresponds with the minimum value of activation energy. The explanation for the enhancement in the conductivity is given on the basis of Anderson and Stuart model. According to this model, as one of the network ions is substituted by another glass modifier ion, the average interionic bond distance becomes larger or smaller according to whether the substituting ion is larger or smaller. In the present case, Dy being slightly larger in size than boron, the substitution of boron by Dy will increase the interionic bond distance. Thus with the addition of 0.4 mol% Dy_2O_3, the structure becomes loose and hence the conductivity increases [32]. The decrease in conductivity beyond 0.8 mol% Dy_2O_3 is similar to that reported in alkali alumino silicate glass system [33]. In the present study, the addition of Dy_2O_3 eliminates the number of non-bridging oxygens (NBOs) and simultaneously creates bridging oxygens (BOs). This may decrease the open structure, through which charge carrier can move with lower mobility [34]. The further enhancement in conductivity may be due to the creation of NBOs.
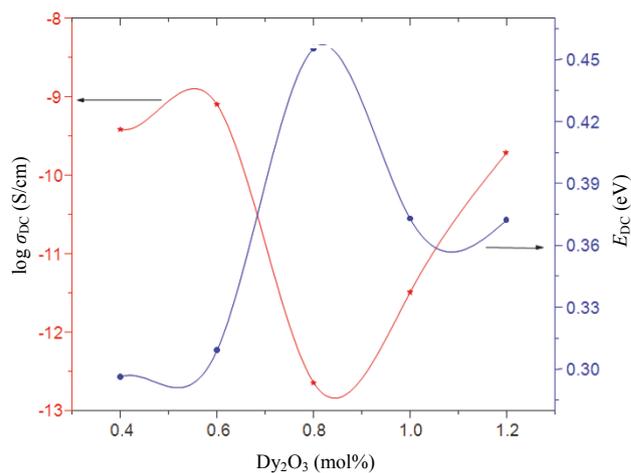
3.3 Transference number measurement

The transference number gives the information of the extent of ionic and electronic contribution to the total conductivity. The total ionic and electronic transference numbers (t_{ion} and t_{ele}) were measured using DC polarization technique by sandwiching the sample between graphite (blocking) electrodes. The polarization current has been monitored as a function of time by applying fixed DC potential across the sample. The total ionic and electronic transference numbers have been calculated from the plot using Eqs. (1) and (2) [22–25].

The current versus time plots of all samples are obtained which exhibit typical behavior of ionic charge transport. Figure 3 shows the plots of current versus time for all the compositions of $60V_2O_5$–$5P_2O_5$–
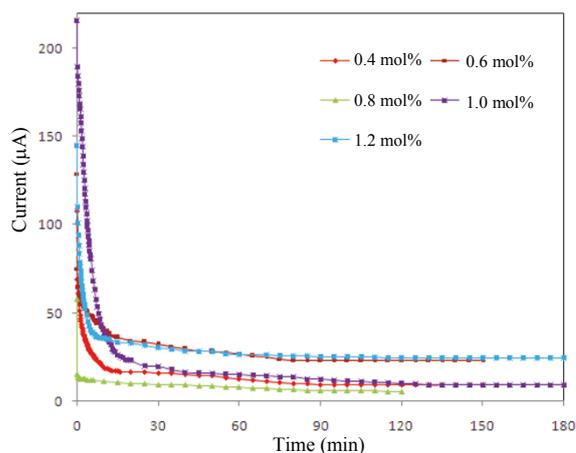

Fig. 3 Plots of DC current versus time for $60V_2O_5$–$5P_2O_5$–$(35-x)B_2O_3$–xDy_2O_3.

$(35-x)B_2O_3-xDy_2O_3$. The total current becomes nearly constant at some non-zero value after some time. The final residual current is mainly due to electrons/holes. The values of transference numbers are found to be in the range of 0.82 to 0.96. This suggests that the charge transport in all the samples are predominantly due to ions.

3.4 Density, molar volume and oxygen packing density

The density is a powerful tool capable of exploring the changes in the structure of glasses. The density is affected by the structural softening/compactness, change in geometrical configuration, coordination number, cross-link density, and dimension of interstitial spaces of the glass. In the studied glasses, it is noted that the density decreases from 2.88 g/cm^3 to 2.74 g/cm^3, congruent with an increase in the molar volume from 49.32 cm^3/mol to 52.36 cm^3/mol as the Dy_2O_3 content increases on the expense of B_2O_3 content as shown in Fig. 4 and listed in Table 1. It is expected that the density and molar volume should show opposite behavior to each other, and so in the studied glasses the molar volume increase with the decrease in the density as the Dy_2O_3 content increases [35]. The increase in the molar volume can be attributed to the larger packing factor of Dy_2O_3 than that of B_2O_3. Accordingly, the structure of the studied glasses will be expanded, but with compactness and high number of covalent bonds. Figure 5 shows the variation of molar volume as well as OPD with Dy_2O_3 content. It is noted that the molar volume increases and OPD decreases with Dy_2O_3 content [36–38].

4 Conclusions

The melt-quenching technique is a very simple method for the preparation of the conducting glasses. The DC conductivity shows Arrhenius-type temperature dependence. The maximum value of conductivity and
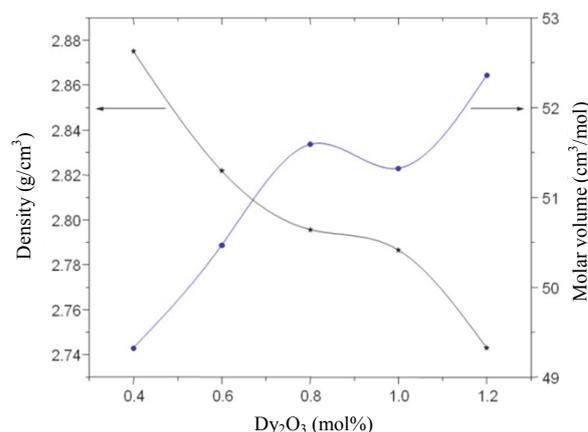

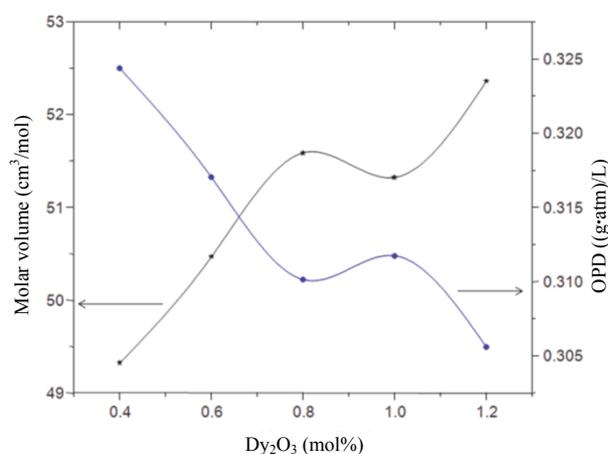Fig. 4 Variation of the density and molar volume with molar fraction of Dy_2O_3.

Fig. 5 Variation of molar volume and OPD with molar fraction of Dy_2O_3.

minimum value of activation energy are found to be in the range of 8.22×10^{-3} S/cm at 473 K and 0.30–0.52 eV, respectively. The ionic conductivity is found to be dominant over the electronic conductivity and varies between 82% and 96%. It is realised that the structural modification depends on the density and molar volume. The density is found to be decreased from 2.88 g/cm^3 to 2.74 g/cm^3, congruent with the increase in molar volume from 49.32 cm^3/mol to 52.36 cm^3/mol as the Dy_2O_3 content increases.

Table 1 Physical properties of 60V$_2$O$_5$–5P$_2$O$_5$–(35–x)B$_2$O$_3$–xDy$_2$O$_3$

Dy_2O_3 (mol%)	Density, ρ (g/cm^3)	Molecular weight, M_T (g/mol)	Molar volume, V_m (cm^3/mol)	OPD, D_O ((g·atm)/L)
0.4	2.88	141.80	49.32	0.320
0.6	2.82	142.41	50.47	0.317
0.8	2.79	144.23	51.59	0.310
1.0	2.78	143.02	51.32	0.311
1.2	2.74	143.63	52.36	0.305

Acknowledgements

References

[1] Al-Hajry A, Soliman AA, El-Desoky MM. Electrical and thermal properties of semiconducting Fe_2O_3–Bi_2O_3–$Na_2B_4O_7$ glasses. *Thermochim Acta* 2005, **427**: 181–186.

[2] El-Desoky MM, Al-Shahrani A. Variable—Range hopping in Fe_2O_3–Bi_2O_3–$K_2B_4O_7$ glasses. *J Mater Sci: Mater El* 2005, **16**: 221–224.

[3] Al-Hajry A, Tashtoush N, El-Desoky MM. Characterization and transport properties of semiconducting Fe_2O_3–Bi_2O_3–$Na_2B_4O_7$ glasses. *Physica B* 2005, **368**: 51–57.

[4] Saddeek YB, Shaaban ER, Aly KA, *et al*. Characterization of some lead vanadate glasses. *J Alloys Compd* 2009, **478**: 447–452.

[5] El-Desoky MM. Small polaron transport in V_2O_5–NiO–TeO_2 glasses. *J Mater Sci: Mater El* 2003, **14**: 215–221.

[6] Al-Shahrani A, Al-Hajry A, El-Desoky MM. Non-adiabatic small polaron hopping conduction in sodium borate tungstate glasses. *Phys Status Solidi a* 2003, **200**: 378–387.

[7] El-Desoky MM, Tashtoush NM, Habib MH. Characterization and electrical properties of semiconducting Fe_2O_3–Bi_2O_3–$K_2B_4O_7$ glasses. *J Mater Sci: Mater El* 2005, **16**: 533–539.

[8] El-Desoky MM, Al-Hajry A, Tokunaga M, *et al*. Effect of sulfur addition on the redox state of iron in iron phosphate glasses. *Hyperfine Interact* 2004, **156–157**: 547–553.

[9] Mahmoud KH, Abdel-Rahim FM, Atef K, *et al*. Dielectric dispersion in lithim–bismuth–borate glasses. *Curr Appl Phys* 2011, **11**: 55–60.

[10] Terczynska-Madej A, Cholewa-Kowalska K, Laczka M. The effect of silicate network modifiers on colour and electron spectra of transition metal ions. *Opt Mater* 2010, **32**: 1456–1462.

[11] Venkat Reddy P, Laxmi Kanth C, Prasanth Kumar V, *et al*. Optical and thermoluminescence properties of R_2O–RF–B_2O_3 glass systems doped with MnO. *J Non-Cryst Solids* 2005, **351**: 3752–3759.

[12] Ramesh Babu A, RajyaSree C, Srinivasa Rao P, *et al*. Vanadyl ions influence on spectroscopic and dielectric properties of glass network. *J Mol Struct* 2011, **1005**: 83–90.

[13] Ramesh Babu A, RajyaSree C, Vinaya Teja PM, *et al*. Influence of manganese ions on spectroscopic and dielectric properties of LiF–SrO–B_2O_3 glasses. *J Non-Cryst Solids* 2012, **358**: 1391–1398.

[14] Srinivasa Rao P, Bala Murali Krishna S, Yusub S, *et al*. Spectroscopic and dielectric investigations of tungsten ions doped zinc bismuth phosphate glass-ceramics. *J Mol Struct* 2013, **1036**: 452–463.

[15] Takahashi H, Karasawa T, Sakuma T, *et al*. Electrical conduction in the vitreous and crystallized Li_2O–V_2O_5–P_2O_5 system. *Solid State Ionics* 2010, **181**: 27–32.

[16] Kiran N, Kesavulu CR, Suresh Kumar A, *et al*. Spectral studies on Cr^{3+} ions doped in sodium–lead borophosphate glasses. *Physica B* 2011, **406**: 1897–1901.

[17] Kim CE, Hwang HC, Yoon MY, *et al*. Fabrication of a high lithium ion conducting lithium borosilicate glass. *J Non-Cryst Solids* 2011, **357**: 2863–2867.

[18] Pisarski WA, Goryczka T, Wodecka-Dus B, *et al*. Structure and properties of rare earth-doped lead borate glasses. *Mat Sci Eng B* 2005, **122**: 94–99.

[19] Qiu J, Igarashi H, Makishima A. Long-lasting phosphorescence in Mn^{2+}:Zn_2GeO_4 crystallites containing transparent GeO_2–B_2O_3–ZnO glass-ceramics. *Sci Technol Adv Mater* 2005, **6**: 431–434.

[20] Barde RV, Waghuley SA. Study of AC electrical properties of V_2O_5–P_2O_5–B_2O_3–Dy_2O_3 glasses. *Ceram Int* 2013, **39**: 6303–6311.

[21] Yoon HJ, Jun DH, Yang JH, *et al*. Carbon dioxide gas sensor using a graphene sheet. *Sensor Actuat B: Chem* 2011, **157**: 310–313.

[22] Sekhon SS, Chandra S. Mixed cation effect in silver borate ion conducting glass. *J Mater Sci* 1999, **34**: 2899–2902.

[23] Das SS, Srivastava V, Singh P. Ionic transport sodium phosphate glasses doped with chloride of Co, Cd and Ag. *Indian J Eng Mater Sci* 2006, **13**: 455–461.

[24] Sheha E. Ionic conductivity and dielectric properties

of plasticized $PVA_{0.7}(LiBr)_{0.3}(H_2SO_4)_{2.7M}$ solid acid membrane and its performance in a magnesium battery. *Solid State Ionics* 2009, **180**: 1575–1579.

[25] Reddy J, Ramesh Ch, Kumar S, *et al*. Conductivity study of PEO complex with Mg^{2+} borate glass polymer electrolyte—Its application as electrochemical cell. *Int J Appl Engng Res Dindigul* 2011, **2**: 147–156.

[26] Govindaraj G, Mariappan CR. Synthesis, characterization and ion dynamic studies of NASICON type glasses. *Solid State Ionics* 2002, **147**: 49–59.

[27] Abid M, Et-tabirou M, Taibi M. Structure and DC conductivity of lead sodium ultraphosphate glasses. *Mat Sci Eng B* 2003, **97**: 20–24.

[28] Mansour E, El-Damrawi GM, Moustafa YM, *et al*. Polaronic conduction in barium borate glasses containing iron oxide. *Physica B* 2001, **293**: 268–275.

[29] Ramadevudu G, Laxmi Srinivasa Rao S, Hameed A, *et al*. FTIR and some physical properties of alkaline earth borate glasses containing heavy metal oxides. *Int J Eng Sci Tech* 2011, **3**: 6998–7005.

[30] Insiripong S, Chimalawong P, Kaewkhao J, *et al*. Optical and physical properties of bismuth borate glasses doped with Dy^{3+}. *Am J Applied Sci* 2011, **8**: 574–578.

[31] Bale S, Rahman S. Spectroscopic and physical properties of Bi_2O_3–B_2O_3–ZnO–Li_2O glasses. *Int Sch Res Netw Spectrosc* 2012, DOI: 10.5402/2012/634571.

[32] Gedam RS, Deshpande VK. An anomalous enhancement in the electrical conductivity of Li_2O: B_2O_3:Al_2O_3 glasses. *Solid State Ionics* 2006, **177**: 2589–2592.

[33] Alexander MN, Onorato PIK, Struck CW, *et al*. Structure of alkali (alumino) silicate glasses: I. Tl^+ luminescence and the nonbridging oxygen issue. *J Non-Cryst Solids* 1986, **79**: 137–154.

[34] El-Desoky MM, Ibrahim FA, Mostafa AG, *et al*. Effect of nanocrystallization on the electrical conductivity enhancement and Mössbauer hyperfine parameters of iron based glasses. *Mater Res Bull* 2010, **45**: 1122–1126.

[35] Abid M, Et-tabirou M, Taibi M. Structure and DC conductivity of lead sodium ultraphosphate glasses. *Mat Sci Eng B* 2003, **97**: 20–24.

[36] Abdel-Baki M, El-Diasty F. Role of oxygen on the optical properties of borate glass doped with ZnO. *J Solid State Chem* 2011, **184**: 2762–2769.

[37] Veeranna Gowda VC, Anavekar RV. Elastic properties and spectroscopic studies of lithium lead borate glasses. *Ionics* 2004, **10**: 103–108.

[38] Silim HA. Composition effect on some physical properties and FTIR spectra of alumino–borate glasses containing lithium, sodium, potassium and barium oxides. *Egypt J Solids* 2006, **29**: 293–301.